AJNR

This information is current as of August 21, 2025.

Gadolinium-DTPA in the Evaluation of Intradural Extramedullary Spinal Disease

Gordon Sze, Andrea Abramson, George Krol, David Liu, Jay Amster, Robert D. Zimmerman and Michael D. F. Deck

AJNR Am J Neuroradiol 1988, 9 (1) 153-163
http://www.ajnr.org/content/9/1/153

Gadolinium-DTPA in the Evaluation of Intradural Extramedullary Spinal Disease

Gordon Sze[1]
Andrea Abramson
George Krol
David Liu
Jay Amster
Robert D. Zimmerman
Michael D. F. Deck

Gadolinium-DTPA was used in MR imaging of the spine to determine the ability of a contrast agent to increase the detection and characterization of disease in the intradural extramedullary space. Although MR imaging, especially with recent technological improvements, has been shown to be at least competitive with, and often superior to, myelography and postmyelography CT in the study of intramedullary and extradural disease, its use in the assessment of intradural extramedullary disease has been questioned. We selected 12 patients with intradural extramedullary disease as demonstrated by positive CSF cytology and/or myelographic findings and performed MR examinations on them before and after administering gadolinium-DTPA (0.1 mmol/kg).

Gadolinium-DTPA was extremely effective in depicting intradural extramedullary disease of the spine. Small nodules of 3 mm, virtually invisible on noncontrast MR scans, enhanced strongly and were easily detected. In addition, leptomeningeal spread of tumor along nerve roots was also visualized, sometimes more readily than by myelography and postmyelography CT. The remarkable sensitivity of gadolinium-DTPA to intradural extramedullary disease assures its role in future MR examinations of the spine.

Early researchers in MR imaging soon realized the potential of this new technique for evaluating the spine [1–6]. With technological improvements, many reports appeared that detailed the effectiveness of MR imaging of the spine. Intramedullary disease, including subtle tumors and syrinxes, could be assessed more completely and noninvasively than with myelography and postmyelography CT [4, 5, 7–10]. Similarly, extradural disease was also well depicted with MR imaging and, again, the competitiveness of this new technique with more traditional imaging methods was often cited [5, 10, 11].

However, there have been very few reports describing the usefulness of MR imaging in evaluating disease of the intradural extramedullary space [12, 13]. Those reports that have dealt with MR evaluation of intradural extramedullary disease have generally depicted sizable meningiomas and neuromas in the cervical and thoracic regions, with secondary displacement of the cord aiding detection of the lesion [5, 10, 13]. However, even these papers acknowledge the difficulty of seeing some lesions, both occasional larger masses and, especially, smaller nodules less than 5 mm [10, 13].

Because of the problems encountered in MR imaging of intradural extramedullary disease, this investigation focused on the use of gadolinium-DTPA as a contrast agent that could potentially enhance MR detection of disease that might otherwise be only poorly defined or that might not be visualized at all.

Materials and Methods

Twelve patients who showed evidence of intradural extramedullary disease were selected to participate in a multicenter protocol designed to examine the use of gadolinium-DTPA in evaluating suspected spinal tumors. The protocol was carried out under the guidelines of the Food and Drug Administration, the Institutional Review Board and Investigational Drug

This article appears in the January/February 1988 issue of *AJNR* and the April 1988 issue of *AJR*.

Received May 6, 1987; accepted after revision September 8, 1987

This work was supported in part by Berlex Laboratories, NJ.

[1] All authors: Memorial Sloan-Kettering Cancer Center and New York Hospital/Cornell Medical Center, New York City. Address reprint requests to G. Sze, Dept. of Medical Imaging, Memorial Sloan-Kettering Cancer Center, 1275 York Ave., New York, NY 10021.

***AJNR* 9:153–163, January/February 1988**
0195–6108/88/0901–0153
© American Society of Neuroradiology

Committee of the Memorial Sloan-Kettering Cancer Center, and the commercial developer of the product (Berlex Laboratories, Inc., NJ). Fully informed consent was obtained from every patient. The enrollment requirements consisted of strong suspicion of spinal tumor, based on other previous studies or on clinical grounds. Each patient underwent a physical examination and blood chemistry and hematology analysis before and after the administration of gadolinium, in accordance with the guidelines of this phase-III clinical trial. Pregnant and nursing women were excluded.

Of the 12 patients, five had carcinomatous meningitis, three had spinal ependymomas with secondary leptomeningeal spread, two had drop metastases from a cerebral glioblastoma, one had a thoracic meningioma, and one had postoperative arachnoiditis. Four lesions were confirmed surgically; six were documented by clinical history, positive CSF cytology, and myelographic findings; and two were proved by relevant clinical history and myelographic findings. The ages of the patients ranged from 19–79 years. There were three women and nine men. Eleven of the 12 patients had a previous myelogram and postmyelographic CT. Of these 11, eight were evaluated within 1 week of their MR examination. Three patients, with stable disease, were evaluated by myelography and postmyelographic CT within 1 month of MR imaging. Myelography was performed from a lumbar approach, using approximately 10 ml of iohexol at a concentration of 240 mg I/ml, except in cases of total block, in which 4 ml were placed. CT was performed on a high-resolution scanner. Contiguous axial 5-mm scans were obtained through the regions of tumor within 3 hr of instillation of intrathecal contrast material.

For all MR imaging, a superconductive magnet operating at 1.5 T was used. Either a rectangular 18 × 30-cm surface coil or a circular 12.5-cm surface coil was used. In the cervical and thoracic spines, 3-mm sagittal sections with an interslice gap of 0.6 mm were obtained. In the lumbosacral region, 3- or 5-mm sagittal sections with an interslice gap of 0.6 mm or 1 mm, respectively, were obtained. Five-millimeter axial scans with an interslice gap of 1 mm were always obtained. The field of view was 24 or 32 cm for sagittal scans and 16 or 20 cm for axial scans, depending on the region involved. The matrix was 256 × 256. Cardiac gating was used in all long TR sagittal examinations, except in two cases in which a previous myelogram indicated a complete block above the region of interest and in one case in which technical difficulties prevented implementation. In the cases of block, the virtual absence of CSF pulsations was thought to preclude the possibility of significant flow-related artifacts. A respiratory-ordered, phase-encoding technique was added in eight cases to decrease respiratory-induced phase-shift effects.

Each patient first had a preliminary MR examination without contrast. This consisted of a T1-weighted sagittal scan, followed by a proton-density and T2-weighted sagittal scan, followed by a T1-weighted axial scan. For T1-weighted sequences, a repetition time (TR) of 600 msec and an echo delay (TE) of 20 msec were used. In cases that received cardiac gating, the actual TR of the long TR sagittal sequence varied with respect to the heart rate. Generally, examinations were gated to every other heart beat in order to obtain a TR of approximately 1500–2000 msec. Nongated sequences used a TR of 2000 msec. Echo delays in all long TR examinations were 35 and 70 msec. Four excitations were used in all short TR sequences, while two excitations were used in all long TR sequences.

After the preliminary sequences were completed, gadolinium-DTPA in a concentration of 0.1 mmol/kg was injected intravenously over the course of 1 min. Scanning was initiated immediately upon completion of the injection. The same sequences as in the precontrast scans were used, and an additional T1-weighted sagittal scan was included at the end. For purposes of comparison between pre- and postcontrast scans, the patients were advised not to more or change position throughout the entire protocol. The scanning time was approximately 84 min. The actual length of the examination varied from 2½–3½ hr. In cases of anxiety or pain, patients were given diazepam, either intravenously or by mouth, or morphine sulfate, intravenously. The T1-weighted sagittal scans were obtained at approximately 5 and 65 min after injection. The T2-weighted sagittal scan was obtained at approximately 25 min after injection. The T1-weighted axial scan was obtained at approximately 50 min after injection. All times were calculated using the midpoint of the relevant sequences.

After completion of the scanning, the MR images were evaluated in two ways:

1. Intensity measurements were performed on normal and diseased tissues. An operator-defined region of interest (ROI) was selected with an interactive cursor. In all cases, the ROI was as large as possible to cover the representative tissue, without including adjacent CSF. At least 10 pixels were used for each ROI. In precontrast examinations, the tumor was often not visualized well on either the T1- or T2-weighted scans. In these cases, because the patients did not move between scans, the appropriate areas were delineated on the basis of the postcontrast scans. Only the largest lesions in these cases were used. The transmit attenuation was always maintained within 0.5 dB between scans. Absolute signal intensities of the lesions, the CSF, and the background were measured for all seven sequences obtained per patient. The ROI for CSF calculations was always placed at approximately the same distance from the surface coil as the lesion in order to minimize artifactual variations in the intensities resulting from signal drop-off at different distances from the center of the coil. Signal intensities for each lesion were measured three separate times. Signal intensities for CSF and background were measured twice. Values in each category were then averaged to calculate the mean. Based on mean signal intensity measurements of the lesion and background, the formula

$$\frac{[\text{lesion (enh)} - \text{background (enh)}] - [\text{lesion (nonenh)} - \text{background (nonenh)}]}{\text{lesion (nonenh)} - \text{background (nonenh)}}$$

was used to determine the percent of enhancement after administration of gadolinium (enh = enhanced, nonenh = nonenhanced). Based on mean signal intensity measurements of the lesion and the surrounding CSF, the formula

$$\frac{\text{lesion (enh or nonenh)} - \text{background (enh or nonenh)}}{\text{CSF (enh or nonenh)} - \text{background (enh or nonenh)}}$$

was used to determine a contrast index. The contrast indexes before and after gadolinium were compared. For example, in case 1, the mean signal intensities in T1-weighted images were: lesion (enh) 1240; lesion (nonenh) 1148; background (enh) 1036; background (nonenh) 1035; CSF (enh) 1076; and CSF (nonenh) 1082. Using these figures, the percent of enhancement was found to be 81% for T1-weighted images. The contrast index before gadolinium was 2.40, and the contrast index after gadolinium was 5.10.

2. The images were carefully evaluated by four neuroradiologists. Precontrast MR scans, postcontrast MR scans, and the myelogram and postmyelographic CT were individually evaluated in that order with reference to possible lesions in the intradural extramedullary space. Specifically, observers were asked to report the presence of any masses, the number of masses seen, and whether the nerve roots were normal. Lesions were scored on a 4-point scale. For precontrast scans, evaluation consisted of: 0 = no visualization, 1 = equivocal visualization, 2 = definite visualization but poor characterization and delineation, 3 = good characterization and delineation. For postcontrast scans, evaluation consisted of: 0 = no enhance-

TABLE 1: Comparison of Cases and Results

Case No.	Age Gender	Diagnosis and Proof	Myelogram and CT	T1 Nonenhanced[a]	T1 Enhanced[b]	T1 % Enhanced	T2 Nonenhanced[a]	T2 Enhanced	T2 % Enhanced
1	29 M	Ependymoma (surgical)	Thickened nerve roots and nodules	1	3	81	0	2	48
2	19 M	Leukemia (CSF cytology)	Negative	0	0	0	0	0	0
3	28 M	Glioblastoma, drop metastases (clinical, myelogram, CSF cytology)	Lower thoracic block, drop metastases, and thickened nerve roots	1	3	79	0	2	31
4	71 M	Ependymoma (surgical)	Large conus and filum lesion creating total block, with multiple drop metastases. ? thickening of nerve roots	1	3	147	1	3	216
5	23 M	Melanoma (clinical, myelogram, CSF cytology)	Local thickening of nerve roots and mild thecal sac distortion, both visible only in the very distal sac	0	1	70	1	0	28
6	60 F	Breast carcinoma (clinical and myelogram)	Mildly thickened nerve roots and multiple nodules	1	3	58	0	2	58
7	21 M	Ependymoma (surgical)	Irregular conus lesion with total block and a few nodules above and below	1	3	104	1	1	11
8	79 M	Meningioma (surgical)	Not available	3	3	127	3	3	17
9	57 M	Lung carcinoma (clinical, myelogram, CSF cytology)	Mildly thickened nerve roots and two nodules	0	3	157	0	1	0
10	37 F	Postoperative arachnoiditis (clinical and myelogram)	Mild distortion of nerve roots in distal sac	2	2	29	2	0	33
11	58 M	Lung carcinoma (clinical, myelogram, CSF cytology)	Large nodule at C2. Multiple small nodules	2 (large nodule) 0 (small nodules)	3 (all nodules)	130	2 (large nodule) 0 (small nodules)	2 (large nodule) 1 (small nodules)	42
12	45 M	Glioblastoma drop metastases (clinical, myelogram, CSF cytology)	Lumbar block, with tumor filling the distal sac	0	3	194	0	2	[c]

[a] 0 = normal, 1 = equivocal findings, 2 = poorly seen lesions with poor characterization and delineation, 3 = well-seen lesions with good characterization and delineation

[b] 0 = no enhancement, 1 = equivocal enhancement (detected only if the precontrast image is available for side-by-side comparison), 2 = definite enhancement, 3 = marked enhancement

[c] Could not be computed because of patient movement between nonenhanced and enhanced scans.

ment, 1 = equivocal enhancement (detected only if the precontrast image was available for side-by-side comparison), 2 = definite enhancement, 3 = marked enhancement and good delineation of lesions.

Results

The results of the studies are presented in Table 1.

Myelography and Postmyelographic CT

Four of the 12 patients showed total myelographic block with thickened nerve roots and multiple nodules of varying sizes in the subarachnoid space at other levels. Four of the 12 patients were found to have thickened nerve roots and small nodules without evidence of block. Two of the 10 patients had minimal or equivocal thickening of nerve roots alone. One of these had mild thecal sac distortion and thickening of the nerve roots localized to one aspect of the very distal thecal sac. Finally, the last patient had a normal myelogram and postmyelographic CT but showed evidence of leptomeningeal spread of tumor through positive CSF cytology alone. One patient did not receive a myelogram.

Precontrast MR—T1-Weighted Images

Four of the 12 patients showed normal T1-weighted MR examinations of the affected region (Fig. 1). Five of the 10 patients exhibited equivocal MR findings (Figs. 2 and 3). These findings included poor visualization of the conus and a faint suggestion of heterogeneity in the intensity of the CSF signal. One patient had definite but poorly delineated lesions, consisting of clumping of nerve roots posteriorly. One patient, with a thoracic meningioma, had a well-seen lesion. This lesion was clearly intradural extramedullary and deviated the cord, although the exact delineation between tumor and cord could not be made. The final patient had a large deposit of tumor easily visualized; however, multiple smaller nodules were not detected.

Precontrast MR—T2-Weighted Images

Six of the 12 patients had normal proton-density and T2-weighted MR examinations (Figs. 4 and 5). Three of the 10 had equivocal findings, with possible nodules seen (Fig. 3). One of the 10 had poorly delineated clumping of nerve roots. One of the 10, again the patient with the meningioma, had a

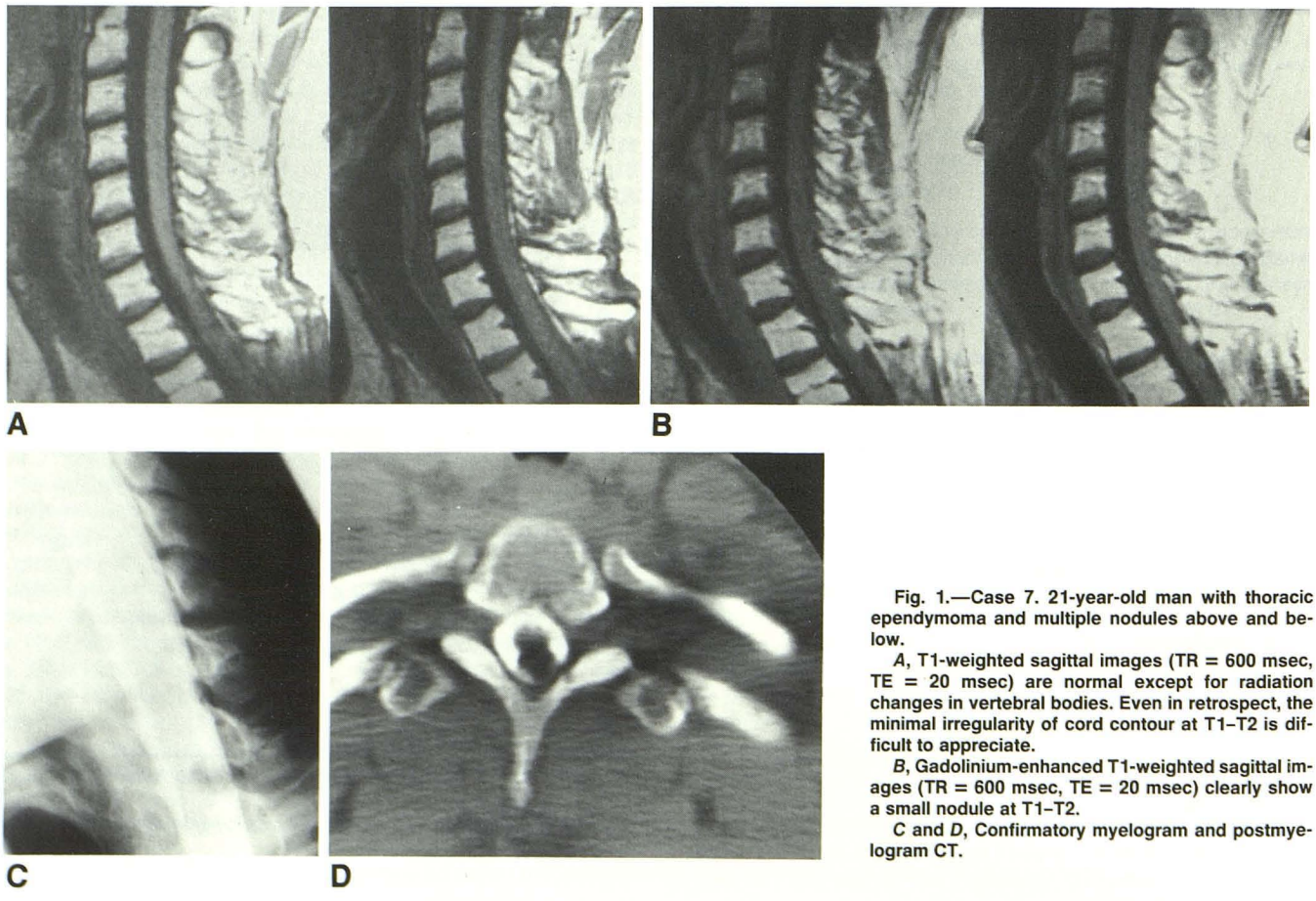

Fig. 1.—Case 7. 21-year-old man with thoracic ependymoma and multiple nodules above and below.

***A*, T1-weighted sagittal images (TR = 600 msec, TE = 20 msec) are normal except for radiation changes in vertebral bodies. Even in retrospect, the minimal irregularity of cord contour at T1–T2 is difficult to appreciate.**

***B*, Gadolinium-enhanced T1-weighted sagittal images (TR = 600 msec, TE = 20 msec) clearly show a small nodule at T1–T2.**

***C* and *D*, Confirmatory myelogram and postmyelogram CT.**

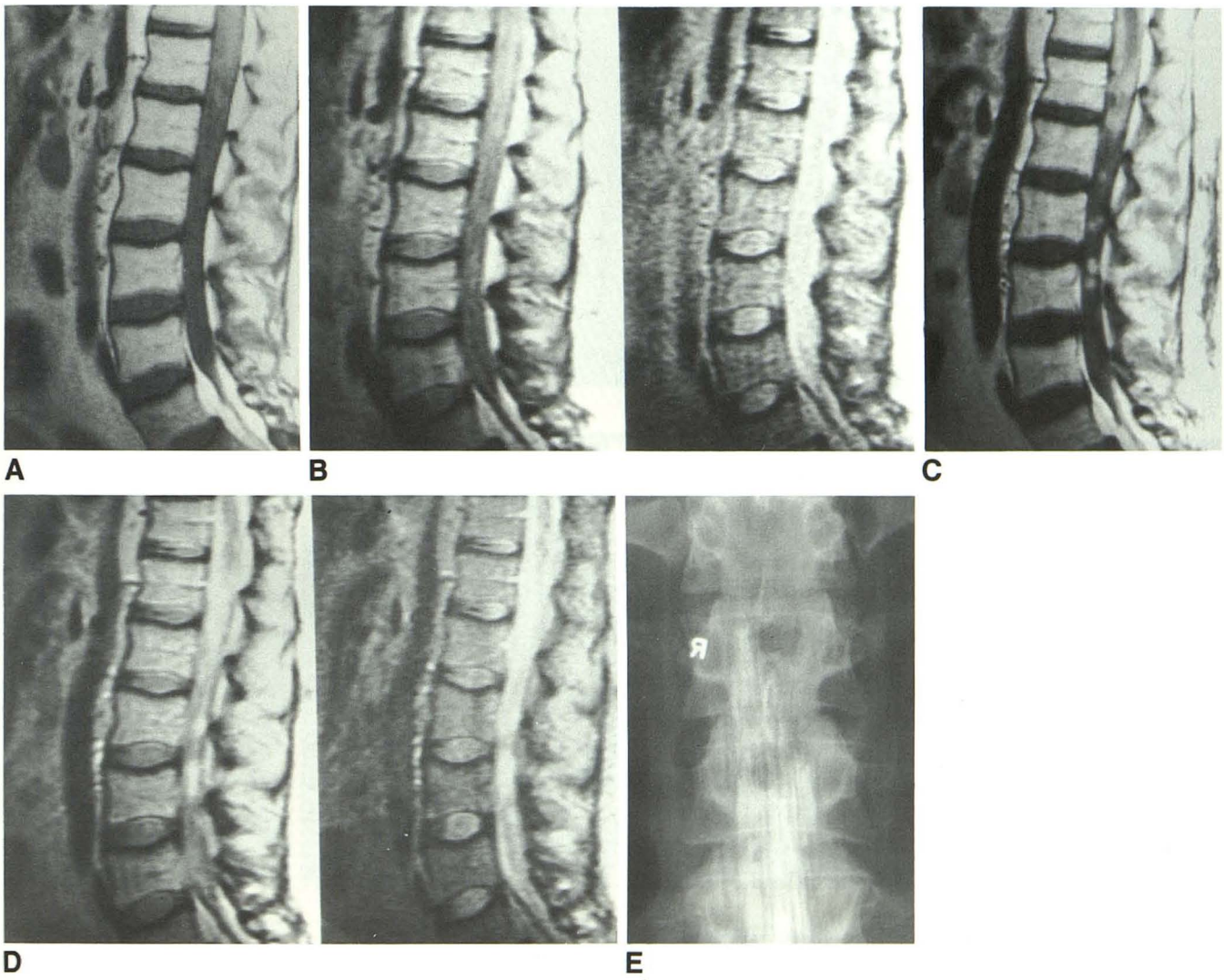

Fig. 2.—Case 3. 28-year-old man with known cerebral glioblastoma, now presenting with bilateral lower extremity weakness and back pain. Clinical diagnosis based on clinical history, myelogram, and positive CSF cytology: drop metastases.

***A*, T1-weighted sagittal scan (TR = 600 msec, TE = 20 msec) is negative except for poor definition of conus and proximal nerve roots. In retrospect only, very vague nodules may be present in subarachnoid space.**

***B*, Proton-density and T2-weighted sagittal scans (TR = 2000 msec, TE = 35/70 msec) are also equivocal. There may be a suggestion of high intensity near conus.**

***C*, T1-weighted sagittal scan (TR = 600 msec, TE = 20 msec) after contrast shows enhancing subarachnoid tumor encasing nonenhancing distal spinal cord, causing the total block seen on myelogram. In addition, multiple other drop metastases are clearly seen.**

***D*, Proton-density and T2-weighted sagittal scans (TR = 2000 msec, TE = 35/70 msec) after contrast show that lesions still enhance, due most likely to persistent contribution of T1 shortening by the gadolinium, even in this long TR sequence.**

***E*, Myelogram confirms presence of multiple nodules and total block at level of conus.**

definite lesion. As with the T1-weighted images, the final patient again had a well-visualized large tumor mass with multiple smaller undetected nodules.

Of incidental note, one of the patients with equivocal findings (case 4) had an additional sagittal sequence performed with a TR of 2500. This examination showed the main conus lesion more clearly and also revealed one small drop metastasis.

Postcontrast MR

Marked contrast enhancement was present in nine of 12 cases (Figs. 1–5). Nodules of all sizes enhanced prominently (Figs. 1–3). Even small drop metastases of 2 or 3 mm were easily seen. In the case in which the additional TR sequence of 2500 msec showed one small drop metastasis, gadolinium enhancement revealed two other drop metastases. In eight

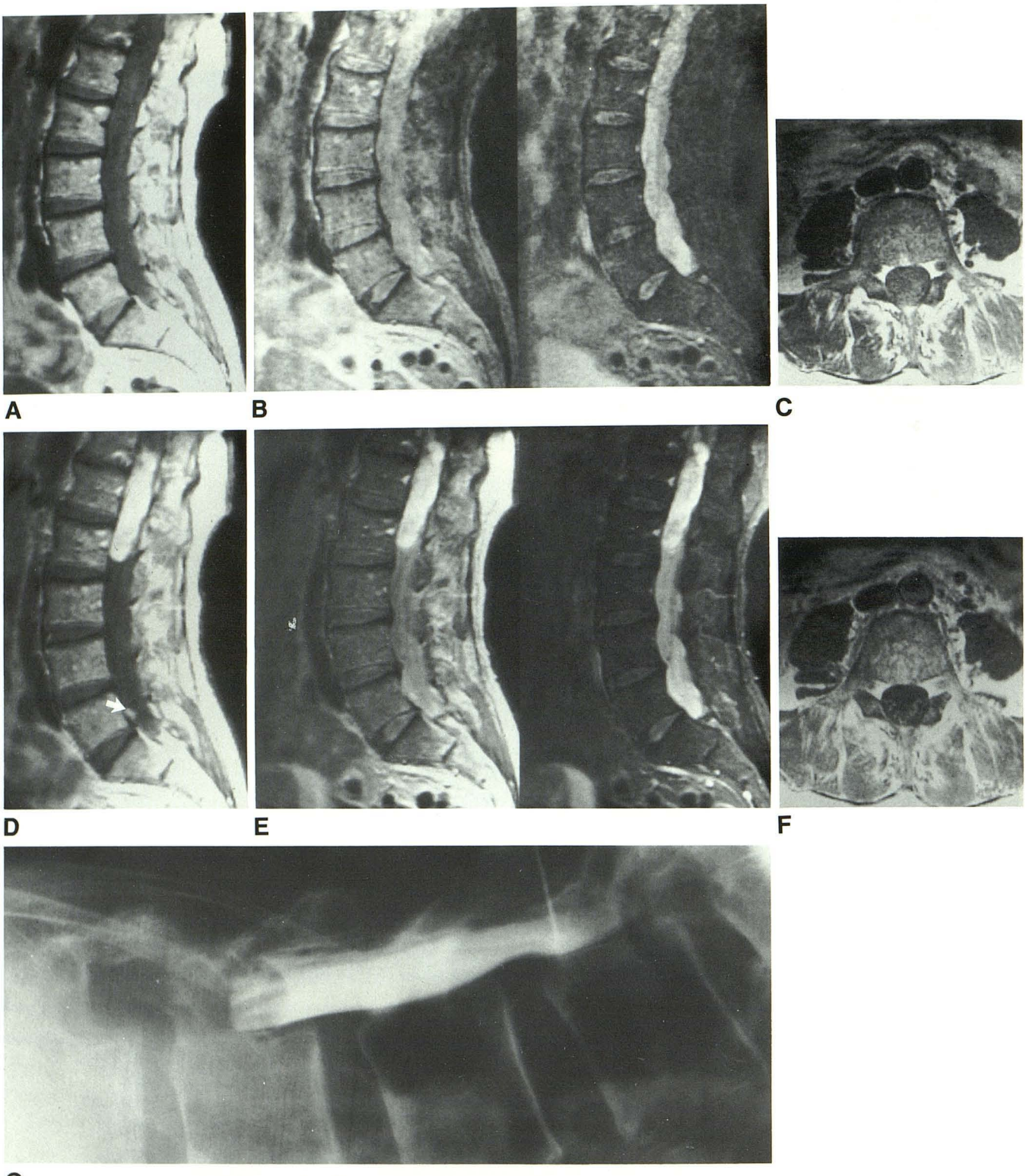

Fig. 3.—Case 4. 71-year-old man with pain and mild weakness in right lower extremity. Surgical pathology: ependymoma.

A, T1-weighted sagittal section (TR = 600 msec, TE = 20 msec) shows normal spinal canal except for lack of clear visualization of conus. No mass is seen.

B, Proton-density and T2-weighted sagittal sections (TR = 2000 msec, TE = 35/70 msec) show a suggestion of heterogeneity in region of conus. Again, no definite mass is seen and no distal lesions are present.

C, T1-weighted axial section (TR = 600 msec, TE = 20 msec) through distal thecal sac is normal. No abnormality of nerve roots is seen.

D, T1-weighted sagittal section (TR = 600 msec, TE = 20 msec) after gadolinium administration shows markedly enhancing conus and filum terminale lesion. In addition, small nodules are evident below (*arrow*).

E, Proton-density and T2-weighted sagittal sections (TR = 2000 msec, TE = 35/70 msec) after gadolinium-DTPA administration show persistent hyperintensity of lesion but less contrast, since tumor is now surrounded by high-intensity CSF.

F, T1-weighted axial section (TR = 600 msec, TE = 20 msec) shows enhancement of all nerve roots. At surgery, leptomeningeal spread of tumor coating all the nerve roots was found.

G, CT myelogram confirms gadolinium MR findings, although nerve roots were not markedly thickened.

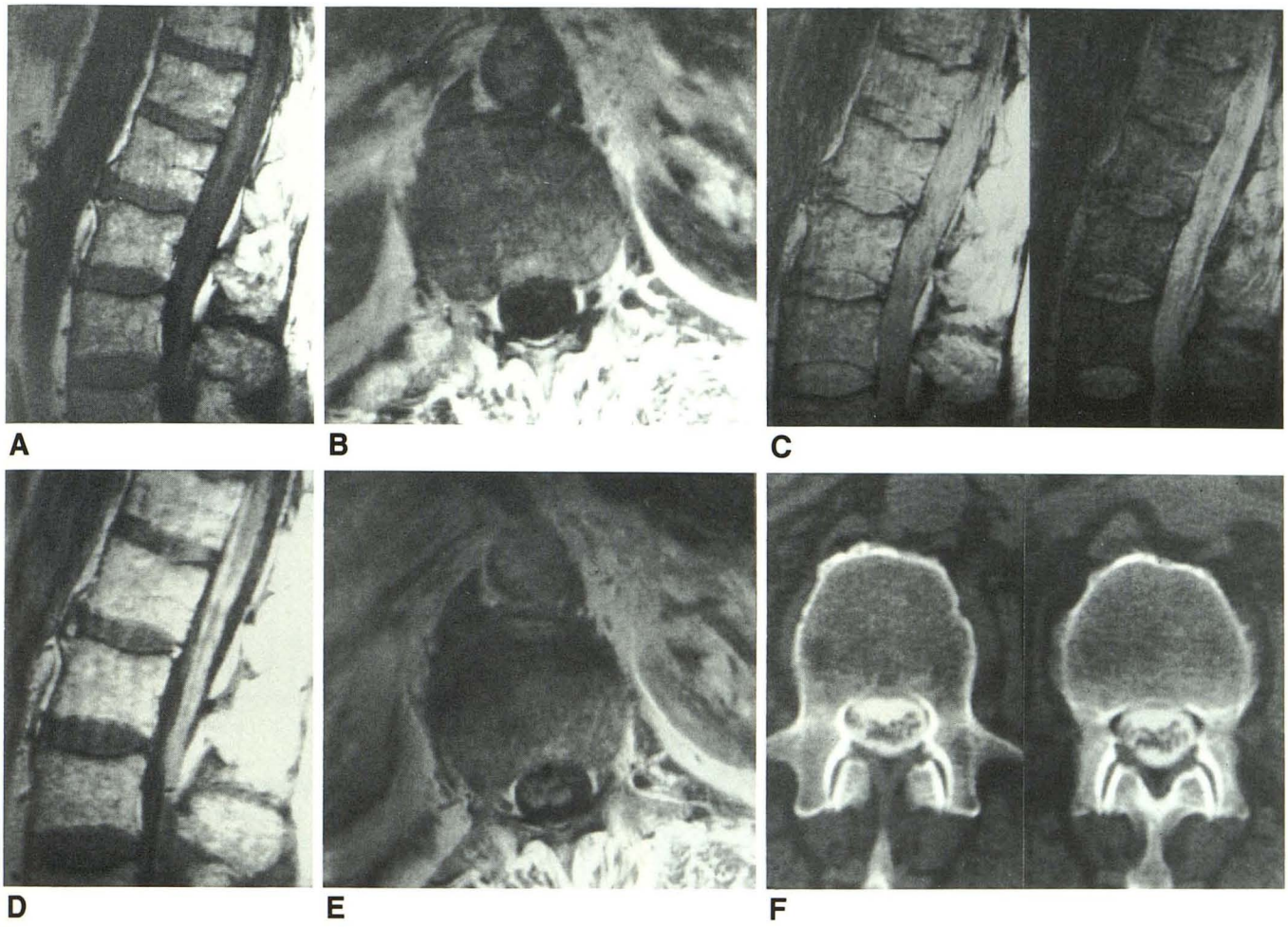

Fig. 4.—Case 9. 57-year-old man with lung carcinoma and lower extremity weakness. Clinical diagnosis based on clinical history, myelogram, and positive CSF cytology: carcinomatous meningitis.

***A* and *B*, Normal T1-weighted sagittal and axial scans (TR = 600 msec, TE = 20 msec) of filum and nerve roots.**

***C*, Proton-density and T2-weighted sagittal scans (TR = 2000 msec, TE = 35/70 msec) add no further information.**

***D* and *E*, Postcontrast T1-weighted sagittal and axial scans (TR = 600 msec, TE = 20 msec) show marked enhancement of all nerve roots. In addition, clumping of nerve roots is present.**

***F*, Postmyelographic CT shows thickening of nerve roots.**

of the nine cases with marked enhancement, the enhancement was so striking that comparison with precontrast images was not necessary. In the ninth case, comparison was useful only to differentiate a small distal sac drop metastasis from lumbar epidural fat. In two cases, the myelogram and postmyelographic CT suggested nerve root thickening and the contrast-enhanced MR showed an extensive enhancement of all the nerve roots (Fig. 4).

Equivocal contrast enhancement was present in one case (case 5). While the myelogram and postmyelographic CT suggested thickening of the nerve roots and mild thecal sac distortion localized only to the distal lumbar region, the MR disclosed enhancement of the nerve roots, visible only in the axial plane of section. After contrast, the nerve roots could be seen to be clumped to one side of the thecal sac.

Another patient with distorted and clumped nerve roots (case 10) showed definite but not marked enhancement. Tethering and distortion of several nerve root groups to form CSF loculations was clearly depicted.

No contrast enhancement was seen in one case (case 2). This patient had a negative myelogram and postmyelographic CT, with the diagnosis of leptomeningeal spread of tumor made only by CSF cytology. However, the MR examination was performed on the thoracic spine and not on the lumbar spine, where improved delineation of nerve roots may have been present.

Intensity Calculations

Calculations of percent of enhancement and contrast indexes before and after administration of gadolinium-DTPA are presented in Table 1 and Figure 6.

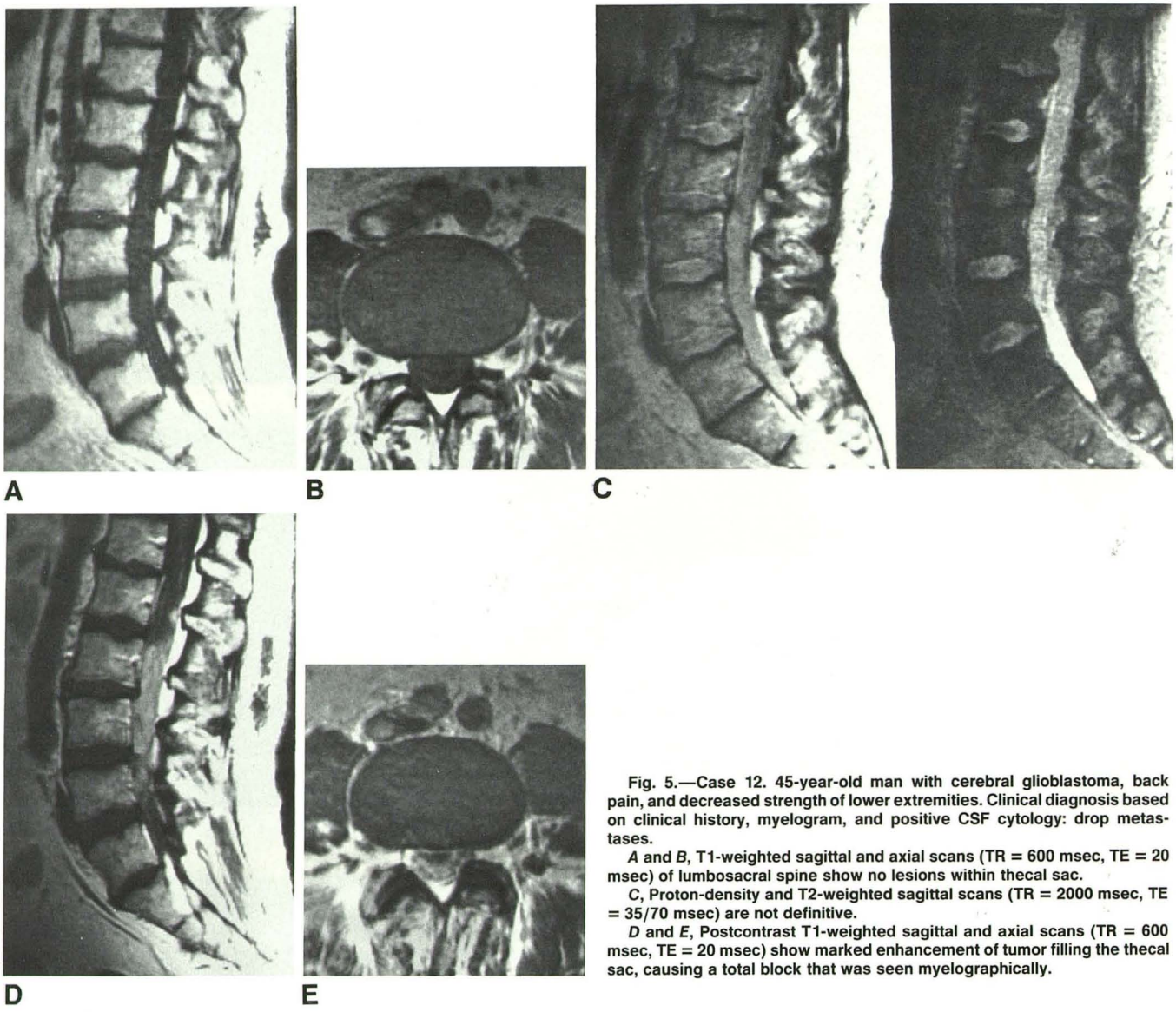

Fig. 5.—Case 12. 45-year-old man with cerebral glioblastoma, back pain, and decreased strength of lower extremities. Clinical diagnosis based on clinical history, myelogram, and positive CSF cytology: drop metastases.

***A* and *B*, T1-weighted sagittal and axial scans (TR = 600 msec, TE = 20 msec) of lumbosacral spine show no lesions within thecal sac.**

***C*, Proton-density and T2-weighted sagittal scans (TR = 2000 msec, TE = 35/70 msec) are not definitive.**

***D* and *E*, Postcontrast T1-weighted sagittal and axial scans (TR = 600 msec, TE = 20 msec) show marked enhancement of tumor filling the thecal sac, causing a total block that was seen myelographically.**

The results for the percent of enhancement for the T1-weighted sequences generally followed expected trends. Lesions that were clearly judged to enhance by the four neuroradiologists who evaluated the cases also showed marked percent of enhancement based on intensity values. The only exceptions (cases 5 and 10) both involved very minimal and localized nerve root thickening. In the first case, the 70% enhancement was thought to be valid but affected only a small clump of nerve roots, easily visible only on axial scans. Thus, the subjective evaluation of the four neuroradiologists was that overall enhancement was only equivocal. In the second case, enhancement of nerve roots was present but these same nerve roots were also visible without contrast. Thus, the percent of enhancement was low. Perhaps the fact that this patient had benign postoperative arachnoiditis rather than tumor contributed to the low enhancement value.

The results for the percent of enhancement for the T2-weighted sequences were much more variable than for the T1-weighted sequences. In large lesions (case 4), enhancement was strong, even in long TR sequences. This persistent effect of gadolinium is most likely due to the larger contribution of T1 weighting with high field strength magnets, compared with low field strength imagers. Further evidence for the importance of the T1 effects even in the long TR sequences can be derived from the fact that the first echo images usually showed the lesions better after administration of gadolinium than did the second echo images. Other cases did not show enhancement on T2-weighted images, probably because of the smaller size of these lesions and the effects of partial voluming of surrounding high-intensity CSF.

The contrast indexes all revealed increased contrast after administration of gadolinium (Fig. 6). In cases with an initial

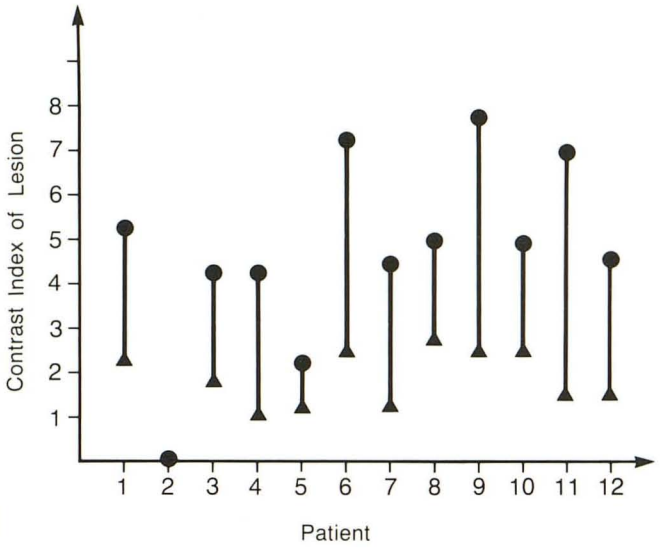

Fig. 6.—Contrast index of lesion on T1-weighted images before (*triangle*) and 5 min after (*circle*) administration of gadolinium-DTPA.

contrast index near 1.0, the lesions were very difficult to see on T1-weighted images. Enhancement in these patients resulted in visualization of the pathology. However, in several cases, the initial contrast index was between 2.0 and 3.5. One fact must be stressed here: Although the lesion was "apparent" on the noncontrast scan, it was not always distinguishable as pathologic. For example, in case 9 (Fig. 4), "normal" nerve roots surrounding the filum were seen initially. However, only after administration of contrast material could the presence of leptomeningeal tumor—confirmed by CSF cytology, myelography, and postmyelographic CT—be assessed. Thus, contrast allowed both visualization of lesions that were otherwise difficult to see and identification of these lesions as abnormal.

Discussion

Considering the sensitivity of noncontrast MR imaging to most disease processes, its frequent failure to adequately depict intradural extramedullary disease in the spine is, at first, surprising. The reasons are probably multiple. First, the relaxation characteristics of these lesions can approach those of the surrounding CSF. Intradural extramedullary disease is characterized by marked elevations of protein levels in the CSF. In addition, subarachnoid spread of tumor is often not compact but rather very delicate, feathering along the nerve roots and forming a "lacy pattern" [14]. Because this disease process does not create well-defined masses but instead amorphous and friable lesions, the spinal cord is often not displaced. The high water content of these disease processes both lowers the T1 relaxation time and raises the T2 relaxation time to resemble those of the proteinaceous CSF. Even extensive tumor spread can often be very poorly delineated on spinal MR imaging. Possibly for these same reasons, meningiomas and neuromas, which tend to form more compact tumor masses and are associated with less marked elevations of protein in the CSF, are easier to visualize on MR than is leptomeningeal tumor spread. However, even in these cases, changes in the relaxation times reflect the higher water content of this diseased tissue than is found in normal tissue. Again, these changes often make it difficult to visualize tumors that are surrounded by CSF [10, 13].

Second, visualization of edema cannot be used to increase sensitivity to detection. Lesions in both the brain and spinal cord are often highlighted by the presence of edema, created by blood brain barrier breakdown and leakage of water into the surrounding parenchyma. Water by itself is a sensitive "contrast agent" in MR imaging [15]. Obviously, such a mechanism cannot operate in the detection of intradural extramedullary disease.

Third, nodules hanging off nerve roots are often very small. Partial voluming of already indistinct lesions can totally obscure them. In addition, just as nerve roots can shift, so the nodules themselves can move with different patient position or with CSF pulsation. This movement may degrade the delineation of the lesions. Furthermore, comparison of lesions in follow-up MR scans can be difficult since the lesions may appear in different positions on two consecutive examinations.

Fourth, well-known technical difficulties often mar interpretation of MR spine images. Movement artifact, both respiratory and cardiac induced, can affect the quality of the most carefully performed examination. Even small amplitudes of CSF motion can prevent detection of lesions, especially those lesions located at the CSF–thecal sac interface [16]. Alternatively, artifactual causes of inhomogeneity in the subarachnoid space can mimic poorly seen and indistinct lesions. CSF flow in the spine is not linear but is usually turbulent, due to the effects of arachnoid septations and nerve roots. Areas of signal heterogeneity often result. In addition, entry phenomena from CSF flow can produce artifacts that may simulate lesions in axial scans of the spine. Cardiac gating and respiratory-ordered, phase-encoding techniques help to a great extent but often do not totally eliminate image degradation [17]. Furthermore, cardiac gating is generally not used in the lumbosacral spine, in T1-weighted images, or in axial scans.

A final obstacle to adequate visualization of intradural extramedullary disease lies in the fact that no consensus has emerged regarding the best pulse sequences to detect small lesions in this space [10, 12, 13]. In our series, short TR sequences were generally more sensitive than long TR sequences, but this was not always the case. In one case (case 4), a very heavily T2-weighted sequence with a TR of 2500 msec was more diagnostic than the routine TR of 2000 msec. However, the longer TR lengthened the examination considerably. Other authors have advocated the use of intermediate-weighted scans to increase sensitivity [10]. We have used repetition times of 1000 and 1500 msec and to date have experienced occasional improvement in the detection of small intradural extramedullary lesions. However, lesions are still difficult to see with these intermediate TRs.

Although gadolinium-DTPA has proved to be effective in

detecting disease in both the head and the spinal cord [18–21], it was initially not necessarily clear how successful it would be in depicting intradural extramedullary disease. Enhancement with any contrast agent is dependent on both blood brain barrier breakdown and an intact blood supply [15]. At best, the blood supply to fragile subarachnoid deposits of tumor must be tenuous. In addition, tumor coating the nerve roots is fine and thin and certainly near the lower limits of resolution of current MR scanners. Even if enhancement occurred, it was unclear that MR would detect these strand-like lesions.

Given all the above considerations, the efficacy and sensitivity of gadolinium-DTPA in depicting even subtle intradural extramedullary disease is truly noteworthy. In one case, tumor coating the bottom of the thecal sac, difficult to detect by traditional techniques, was very apparent after contrast. Even in the case of meningioma, well seen without gadolinium, the application of contrast allowed better differentiation of tumor from cord. In several other cases, marked enhancement of tumor spreading along nerve roots was seen when these changes were only minimally visible on the myelogram and postmyelographic CT. In one case, this visualization enabled a revised preoperative diagnosis of ependymoma to be made over the original diagnosis, based on traditional techniques, of neurofibroma (Fig. 3). Even the case without contrast enhancement must be approached with caution. If the MR scan had been performed of the lumbar rather than the thoracic spine, perhaps nerve root enhancement would have been appreciated. Finally, in one case of melanoma, not included in this series since the gadolinium was given to assess extradural disease and we were not aware of intradural extramedullary lesions, two small enhancing nodules were incidentally noted within the thecal sac. At this time, the CSF protein was normal and the CSF cytology was negative. Retrospective review of the myelogram showed that one lesion was poorly seen; the other was not visualized at all. However, repeat CSF cytology was positive for leptomeningeal spread of tumor.

To date, we have not performed any spine MR studies after administering gadolinium to normal patients. However, we have noted minimal nerve root enhancement in cases of tumor confined to the vertebral bodies without significant thecal sac impingement. Therefore, presumably normal nerve roots do in our experience show mild increase in signal after contrast is given. This fact is not surprising considering that previous work in the head with gadolinium has shown enhancement of the cranial nerves III–VI in their intracavernous portions [22]. The enhancement of normal nerve roots in the thecal sac is difficult to see and is apparent only if the precontrast image is available for side-by-side comparison with the postcontrast image. In subtle cases, such as case 5, the minimal enhancement present may be difficult to differentiate from normal nerve root enhancement. However, in all the remaining positive cases included in this paper, enhancement was easily seen to be more striking than in normal nerve root enhancement. In addition, in several patients with leptomeningeal disease, gadolinium allowed visualization of abnormal thickening of individual nerve roots and clumping of the roots, changes that would be pathologic even if questions remained regarding the degree of enhancement (Fig. 4).

Certain issues did arise peculiar to contrast use in spinal imaging. Especially in the lumbosacral region, extradural fat deposits are almost always present. These fat deposits, especially in the very distal sac, may be difficult to differentiate from enhancement of tumor. Therefore, patient cooperation is even more important in contrast MR imaging of the spine than it is of the head. Identical sections must be compared before and after contrast to rule out lesions near the epidural fat. Therefore, if small lesions are a consideration, especially in the distal thecal sac, patients should not move between scans. Obviously, patient movement precludes the necessary comparison. In very ill patients or in pediatric patients, this restriction may prove difficult. Interestingly, these same issues will most likely arise in gadolinium enhancement of MR imaging in the vertebral bodies and in the head and neck, in which disease is often defined by surrounding fat, whether in the marrow or in the subcutaneous tissues. Further research will indicate whether the enhancement of disease in these regions will actually obscure some lesions.

An additional issue is raised by the length of the contrast MR examinations. Certainly, the time required for these studies was prolonged in order to satisfy the protocol requirements, such as additional sequences and measurements of vital signs. Thus, the length of the examination can undoubtedly be significantly reduced in the future. In evaluating the question of intradural extramedullary disease, T1-weighted sagittal scans before and after contrast are most likely sufficient, unless subtle subarachnoid spread of tumor is a consideration, in which case T1-weighted axial scans may also be of help. With this truncated protocol, the examination can eventually be limited to at most 40 min of imaging time. Unlike imaging of the brain, in which some authors advocate precontrast T2-weighted images even if gadolinium enhancement is used [15], it is doubtful that T2-weighted images in the spine will add any information to the enhanced T1-weighted images in the evaluation of intradural extramedullary disease. Thus, gadolinium-DTPA may indeed help speed patient throughput. (However, if intramedullary lesions, such as multiple sclerosis, are a consideration, then T2-weighted scans will still be required.)

The unusual characteristics of intradural extramedullary disease make it unlikely that "fast scans" will prove of great help in future contrast examinations. As repetition times decrease, residual transverse magnetization increases at the time of the next 90° pulse. Conversion of this residual transverse magnetization into longitudinal magnetization with the subsequent excitation pulse results in greater signal strength from protons with long T2 (and, hence, long T2*) relaxation times [23]. In fact, gradient echo acquisitions are useful precisely because of the high signal generated by CSF [24]. However, disease in the intradural extramedullary space may actually be obscured by these sequences. Again, the peculiarities of intradural extramedullary disease may preclude approaches that may be of use in other anatomic regions. Relative T1 weighting with gradient echo acquisitions can be obtained by increasing the TR and the flip angle, but this

approach minimizes the time-saving advantages of "fast scans" without providing the signal-to-noise levels of regular spin-echo imaging.

Because of the demonstrated sensitivity of gadolinium-enhanced MR scans to small lesions that might otherwise not be detected by MR imaging, the extent of its use in the spine may ultimately be determined not by efficacy but by economics. Millions of patients complain of lower back pain, generally due to degenerative changes and disk disease. However, small neurofibromas and other neoplasms can present very similarly, with nonspecific symptoms. Whether gadolinium-DTPA should be used routinely in these patients in order to detect the occasional case of spinal tumor will be an interesting question for future evaluation. Of incidental note, demand for contrast in our series was very strong on the part of the referring clinicians when they were shown the results of the pre- and postgadolinium studies. Clinical demands, too, may play a role in the future use of MR contrast agents.

In conclusion, gadolinium-DTPA proved extremely effective in depicting intradural extramedullary disease of the spine. These results are particularly noteworthy in view of the lack of visualization of the disease with standard noncontrast MR scans. Unlike the situation in the brain, in which some authors have suggested that precontrast T2-weighted images may be more sensitive than postcontrast T1-weighted images, in the evaluation of possible disease in the intradural extramedullary space, little room for disagreement exists. Contrast-enhanced MR scans in our study were far superior to studies performed without contrast. Because of these facts, the role of contrast in MR examinations of the spine seems assured.

ACKNOWLEDGMENTS

We thank Patricia Dudley for secretarial help and Bruce Peters, Nicole Baccon, and Noreen O'Donnell for technological assistance.

REFERENCES

1. Hans JS, Kaufman B, El Yousef SJ, et al. NMR imaging of the spine. *AJNR* **1983**;4:1151–1159
2. Spinos E, Laster DW, Moody DM, Ball MR, Witcofski RL, Kelly DI. MR evaluation of Chiari I malformations at 0.15 T. *AJNR* **1985**;6:203–208
3. Han JS, Benson JE, Kaufman B, et al. Demonstration of diastematomyelia and associated abnormalities with MR imaging. *AJNR* **1985**;6:215–219
4. Lee BCP, Zimmerman RD, Manning JJ, Deck MDF. MR imaging of syringomyelia and hydromyelia. *AJNR* **1985**;6:221–228
5. Hyman RA, Edwards JH, Vacirca SJ, Stein HL. 0.6 T MR imaging of the cervical spine: multislice and multiecho technique. *AJNR* **1985**;6:229–236
6. Maravilla KR, Lesh P, Weinreb JC, Selby DK, Mooney V. Magnetic resonance imaging of the lumbar spine with CT correlation. *AJNR* **1985**;6:237–245
7. Goy AM, Pinto RS, Raghavendra B, Epstein FJ, Kricheff II. Intramedullary spinal cord tumors: MR imaging, with emphasis on associated cysts. *Radiology* **1986**;161:381–386
8. Kucharczyk W, Brant-Zawadzki M, Sobel D, et al. Central nervous system tumors in children: detection by magnetic resonance imaging. *Radiology* **1985**;155:131–136
9. Di Chiro G, Doppman JL, Dwyer AJ, et al. Tumors and arteriovenous malformations of the spinal cord: assessment using MR. *Radiology* **1985**;156:689–697
10. Modic MT, Masaryk T, Paushter D. Magnetic resonance imaging of the spine. *Radiol Clin North Am* **1986**;24:229–245
11. Norman D, Mills C, Brant-Zawadzki M, Yeates A, Crooks LE, Kaufman L. Magnetic resonance imaging of the spinal cord and canal: potential and limitations. *AJNR* **1984**;5:9–14
12. Barloon TJ, Yuh WTC, Yang CJC, Schultz DH. Spinal subarachnoid tumor seeding from intracranial metastasis: MR findings. *J Comput Assist Tomogr* **1987**;11(2):242–244
13. Scotti G, Scialfa, G, Colombo N, Landoni L. MR imaging of intradural extramedullary tumors of the cervical spine. *J Comput Assist Tomogr* **1985**;9(6):1037–1041
14. Rubinstein LJ. Tumors of the central nervous system. *Atlas of tumor pathology*, second series. Washington, DC: Armed Forces Institute of Pathology, **1972**:325
15. Brant-Zawadzki M, Berry I, Osaki L, Brasch R, Murovic J, Norman D. Gd-DTPA in clinical MR of the brain: I. Intraaxial lesions. *AJNR* **1986**;7:781–788
16. Rubin JB, Enzmann DR. Imaging of spinal CSF pulsation by 2DFT MR: significance during clinical imaging. *AJNR* **1987**;8:297–306
17. Enzmann DR, Rubin JB, Wright A. Use of cerebral fluid gating to improve T2-weighted images. Part I. The spinal cord. *Radiology* **1987**;162:763–767
18. Bydder GM, Brown J, Niendorf HP, Young IR. Enhancement of cervical intraspinal tumors in MR imaging with intravenous gadolinium-DTPA. *J Comput Assist Tomogr* **1985**;9(5):847–851
19. Graif M, Bydder GM, Steiner RE, Niendorf HP, Thomas DGT, Young IR. Contrast-enhanced MR imaging of malignant brain tumors. *AJNR* **1985**;6:855–862
20. Virapongse C, Mancuso A, Quisling R. Human brain infarcts: Gd-DTPA-enhanced MR imaging. *Radiology* **1986**;161:785–794
21. Berry I, Brant-Zawadzki M, Osaki L, Brasch R, Murovic J, Newton TH. Gd-DTPA in clinical MR of the brain: 2. Extraaxial lesions and normal structures. *AJNR* **1986**;7:789–793
22. Kilgore DP, Breger RK, Daniels DL, Pojunas KW, Williams AL, Haughton VM. Cranial tissues: normal MR appearance after intravenous injection of gadolinium-DTPA. *Radiology* **1986**;160:757–761
23. Perkins TG, Wehrli FW. CSF signal enhancement in short TR gradient echo images. *Mag Reson Imag* **1986**;4:465–467
24. Enzmann DR, Rubin JB, Wright A. Cervical spine MR imaging: generating high-signal CSF in sagittal and axial images. *Radiology* **1987**;163:233–238